PHOTOCHEMISTRY AND MAGNETOCHEMISTRY

Effect of Inorganic Anions on the Photochemical Destruction of Azo Dyes

M. R. Sizykh[a], A. A. Batoeva[a,*], and V. A. Munkoeva[a]

*[a] Baikal Institute of Nature Management, Siberian Branch,
Russian Academy of Sciences, Ulan-Ude, 670047 Russia*

*e-mail: abat@binm.ru

Abstract—The effect anions (hydrocarbonates, chlorides, nitrates, and sulfates) have on the kinetics of oxidation of methyl orange in a combined $UV/S_2O_8^{2-}/Fe^{2+}$ system is studied using the UV radiation of a KrCl exilamp (222 nm). Adding hydrocarbonates and nitrates to a solution inhibits the mineralization of dissolved organic carbon. Mineralization degree grows from 31 to 60% in the presence of chlorides (10 mM) and sulfates (1−100 mM). Oxidation is inhibited greatly in real aqueous matrices (natural water and waste water from fur dyeing). In natural surface water, this is mainly due to the effect of hydrocarbonates; in waste water, it is caused by the multicomponent pattern of an aqueous matrix containing process impurities.

INTRODUCTION

Advanced oxidation processes (AOPs) based on photolysis, sonication, ozonation, catalytic systems, and combinations of them are highly efficient in removing toxic and bioresistant pollutants of different chemical natures [1−5]. When using AOPs, many resistant organic substances are oxidized to nontoxic compounds and ultimately mineralized to CO_2 and H_2O [1, 2, 6−8]. Hydroxyl radicals are typically the main reactive oxygen species (ROSes) that participate in oxidation [4]. However, the nonselectivity of OH radicals and the high rates of their reactions with both target compounds and components of real aqueous matrices are limiting factors in using AOPs based on them [9, 10]. Researchers are therefore giving more attention to oxidation systems in which highly reactive sulfate radical anions (E_0 = 2.5−3.1 V), characterized by selectivity [11, 12] and longer lives in solution (30−40 µs) [11] are the main ROSes.

Sulfate radical anions are produced in solutions upon the activation of persulfates or peroxymonosulfates by ultraviolet (UV) radiation, ultrasonic or heat treatment, reactions with transition metal ions or some organic compounds, and in strongly alkaline media [13, 14]. Photochemical processes are easy to induce and allow the highly efficient degradation of organic compounds. Additional use of transition metal catalysts increases the rate of oxidation of pollutants and their mineralization [15].

Sources of UV radiation are usually low-pressure mercury lamps (λ_{max} = 254 nm). However, the global trend toward reducing the industrial and household use of mercury has stimulated the development of new UV sources, including exilamps and light-emitting diode lamps [16, 17]. Gas-discharge exilamps have spectra with narrow emission bands, and are therefore referred to as quasi-monochromatic.

Analysis of the literature data [9, 10, 18−20] shows that the degree and pattern of the effect the components of real aqueous matrices have on the oxidative destruction of organic compounds in combined systems using persulfates as oxidants is governed not only by the nature of the pollutants to be removed, but by how the persulfate is activated as well. In [21], we demonstrated the great effectiveness of the quasi-monochromatic UV radiation of a KrCl exilamp (λ_{max} = 222 nm) when activating persulfate in the oxidative destruction of azo dyes. This work is a continuation of that study. Our aim was to examine the effect the anions most typical of natural and waste waters (hydrocarbonates, chlorides, nitrates, and sulfates) have on the kinetics of the photochemical destruction of azo dyes in a combined Fenton-like $UV/S_2O_8^{2-}/Fe^{2+}$ oxidation system.

Table 1. Effect of hydrocarbonates on the oxidation of MO in the combined $UV/S_2O_8^{2-}/Fe^{2+}$ system; $[Fe^{2+}] = 180\ \mu M$, $[S_2O_8^{2-}] = 180\ \mu M$, and the radiation dose was $1.48\ J\ cm^{-2}$

HCO_3^-, mM	W_0, $\mu M\ min^{-1}$	X, %	$pH_{init}-pH_{fin}$
0	6.1	100	5.4–3.5
1	2.3	83	6.2–6.6
10	2.3	80	7.8–8.2
50	2.3	67	8.3–8.5
100	2.2	60	8.5–8.7

X is the efficiency of oxidation.

EXPERIMENTAL

This work was performed using solutions of methyl orange (sodium 4-(4-dimethylaminophenylazo)benzenesulfonate) with a concentration of 30 μM prepared in different aqueous matrices:

• distilled water (pH 5.7 ± 0.2; specific conductivity, 2 μS cm^{-1});

• natural surface water from the Selenga river (pH 8.3 ± 0.2; HCO_3^- 76.25 ± 9.15 mg/L, Cl^- 1.30 ± 0.17 mg/L, NO_3^- 0.205 ± 0.037 mg/L, SO_4^{2-} 11.27 ± 1.47 mg/L; Fe_{tot} 0.372 ± 0.089 mg/L, COD 31 ± 9.3 mg/L O_2, dissolved organic carbon (DOC) 6.25 ± 1.25 mg/L);

• waste water (wash water from dyeing fur) (pH 2.7, COD 420 mg/L O_2, DOC 210 mg/L).

The concentration of anions was varied in the range of 1−100 mM.

Our experiments on the effect of anions in model aqueous solutions prepared in distilled water were performed under optimum conditions determined earlier for the destruction of methyl orange (MO) in a combined $UV/S_2O_8^{2-}/Fe^{2+}$ system with $[Fe^{2+}]$: $[MO]$: $[S_2O_8^{2-}]$ = 6 : 1 : 6, without adjusting the pH of the medium [21].

The initial pH of the natural water medium was adjusted with 0.1% sulfuric acid.

Our studies were performed using the experimental setup described in [21]. The radiation source was a KrCl exilamp (λ_{max} = 222 nm, 23 W; the KrCl_BD_P model produced by Eksilamps, Russia) with an absorbed radiation intensity of 0.82 mW cm^{-2}, as measured by chemical actinometry with atrazine [22].

The following reagents were used: methyl orange (99.9%, Merck, Germany), potassium persulfate (>99%, Sigma−Aldrich, United States), iron(II) sulfate (100%, Scharlab, Spain), sodium sulfate, sodium chloride, sodium nitrate, and sodium carbonate (Khimreaktivsnab, Russia). The pH of the medium

was measured using a portable Multi3410 instrument with a SenTix®940(WTW) electrode. The concentration of the dye in each solution was controlled via HPLC using an Agilent 1260 Infinity unit equipped with a diode-array UV detector, and a Zorbax SB-C18 column (4.6 × 150 mm). The injection volume was 50 μL, the temperature was 35°C, and the eluent was acetonitrile : 75 mM acetic acid (40 : 60). The flow rate was 0.5 mL/min. Prior to analysis, samples were adjusted to pH 7−8 using 0.1% NaOH and run through a FMPTFE-0.45 μm membrane filter (Vladisart, Russia).

The concentration of the dye in the waste water was determined via spectrophotometry at the characteristic wavelength of 463 nm.

The mineralization degree of organic substrates was estimated from the change in the content of dissolved organic carbon as determined on a Shimadzu TOC-L CSN unit (limit of detection, 50 μg L^{-1}). The instrument was calibrated using reference samples of potassium biphthalate and sodium bicarbonate.

The efficiency of oxidation and mineralization degree were determined from the change in the concentration of methyl orange (MO) and DOC in a treated solution, using the formula

$$E(\%) = \left(1 - \frac{C_\tau}{C_0}\right) \times 100,$$

where C_0 and C_τ are the initial concentrations of MO or DOC and their concentrations at time τ (min), respectively.

The COD value was determined with potassium dichromate. The samples were oxidized in a DRB200 COD reactor (Hach, Germany) with direct recording of the data using a DR-890 portable colorimeter (Hach, Germany).

RESULTS AND DISCUSSION

Effects of Anions

Hydrocarbonates, chlorides, nitrates, and sulfates are typical components of aqueous matrices (natural and waste waters) that affect the kinetics and efficiency of the oxidative destruction of organic compounds.

Hydrocarbonates are known to react at high rates with almost all radicals, and thus have a considerable effect on the efficiency of combined oxidation processes [23]. It has been established experimentally that hydrocarbonates in the considered range of concentrations (1−100 mM) largely inhibits the oxidation of methyl orange in the $UV/S_2O_8^{2-}/Fe^{2+}$ system (Fig. 1). In the presence of hydrocarbonates, the initial rate of oxidation (W_0) of the target compound went from 6.1 to 2.3 μM min^{-1} (by 2.6 times). The efficiency of oxidation of MO fell from 100 to 60%, and no mineralization of DOC was observed (Table 1).
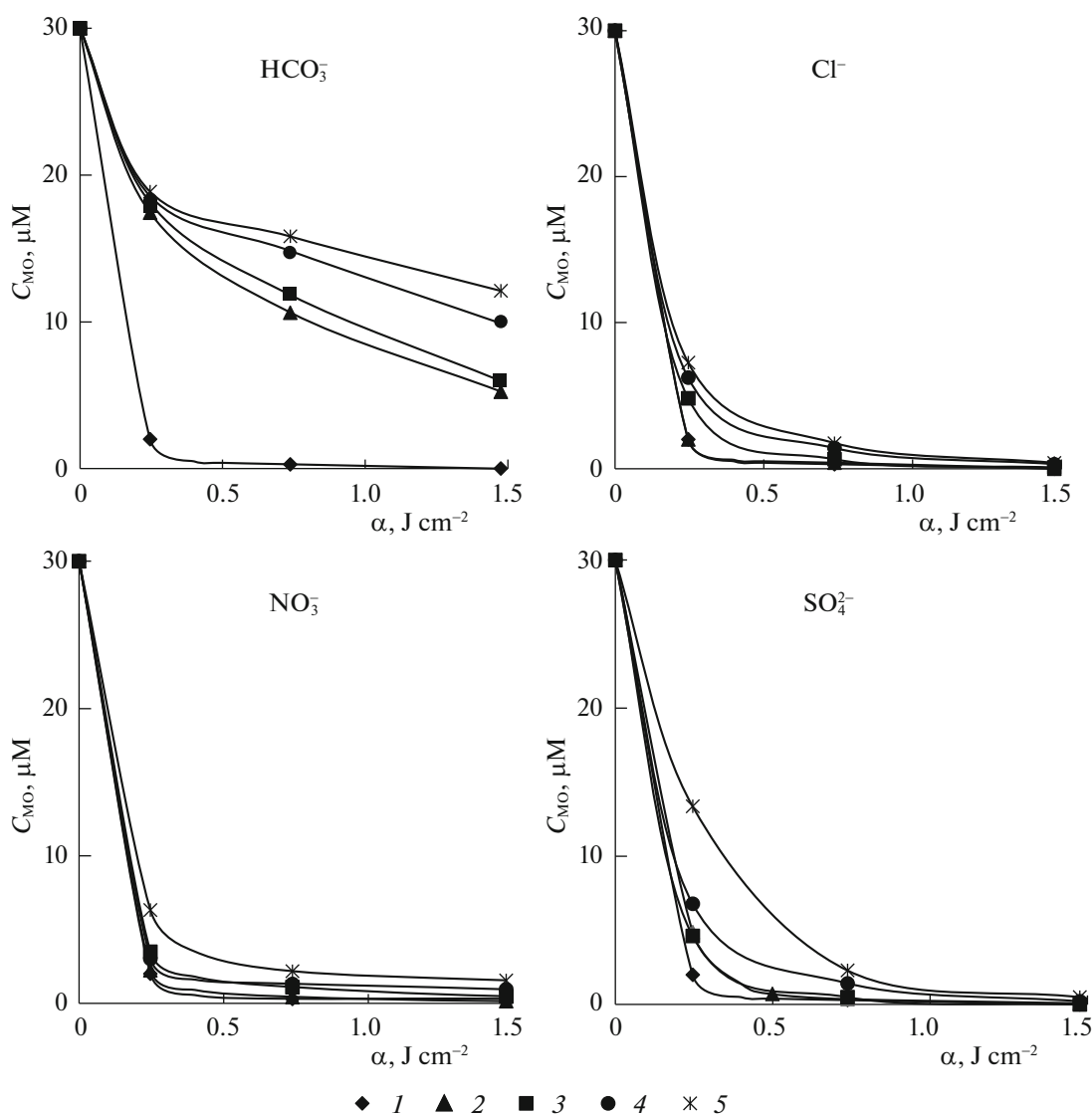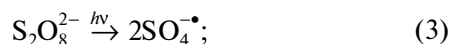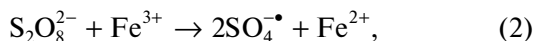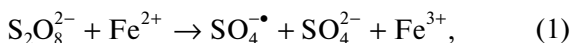
Fig. 1. Effect of anions on the oxidation of methyl orange in the combined $UV/S_2O_8^{2-}/Fe^{2+}$ system: $[Fe^{2+}] = 180\,\mu M$; $[S_2O_8^{2-}] = 180\,\mu M$. The concentrations of anions are (*1*) 0, (*2*) 1, (*3*) 10, (*4*) 50, and (*5*) 100 mM. C_{MO} is the concentration of MO, and α is the radiation dose.

A conjugated radical chain mechanism with the participation of both sulfate radical anions and hydroxyl radicals [21] is observed when MO is oxidized in the $UV/S_2O_8^{2-}/Fe^{2+}$ system. It includes the activation of persulfate with Fe^{2+} and UV radiation,

$$S_2O_8^{2-} + Fe^{2+} \rightarrow SO_4^{-\bullet} + SO_4^{2-} + Fe^{3+}, \quad (1)$$

$$S_2O_8^{2-} + Fe^{3+} \rightarrow 2SO_4^{-\bullet} + Fe^{2+}, \quad (2)$$

$$S_2O_8^{2-} \xrightarrow{h\nu} 2SO_4^{-\bullet}; \quad (3)$$

the photoreduction of Fe^{3+} from hydroxo- and organic complexes; and the formation of $HO^\bullet$ radicals [24, 25]:

$$SO_4^{-\bullet} + H_2O \rightarrow {}^\bullet OH + HSO_4^-, \quad (4)$$

$$Fe^{3+} + H_2O \rightarrow FeOH^{2+} + H^+, \quad (5)$$

$$Fe^{3+} + (OOCR)^- \rightarrow Fe(OOCR)^{2+}, \quad (6)$$

$$FeOH^{2+} \xrightarrow{h\nu} Fe^{2+} + {}^\bullet OH, \quad (7)$$

$$Fe(OOCR)^{2+} \xrightarrow{h\nu} Fe^{2+} + CO_2 + R^\bullet, \quad (8)$$
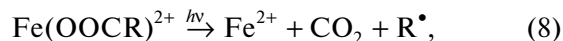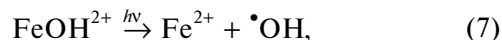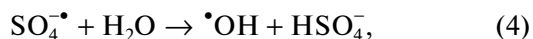
where $Fe(OOCR)^{2+}$ are organometallic complexes with carboxylic acids that form in a solution upon the oxidation of MO.

The target compound and intermediates also undergo direct photolysis reactions:
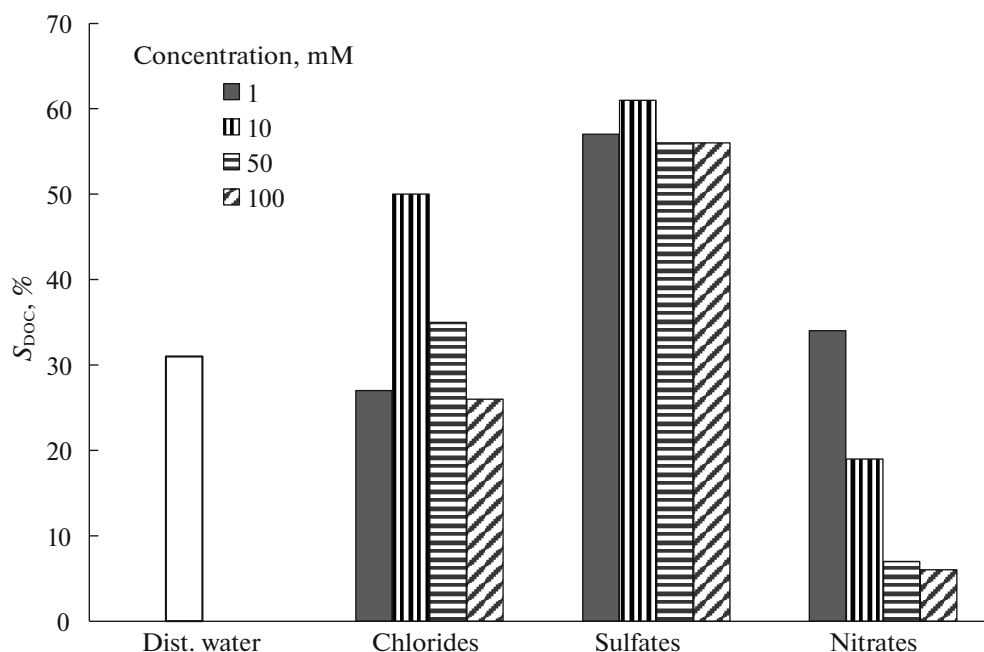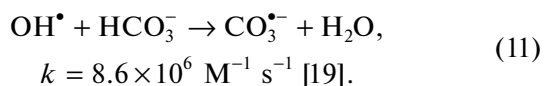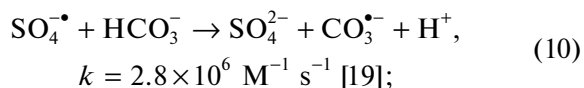
$$MO \xrightarrow{h\nu} \text{intermediates.} \quad (9)$$
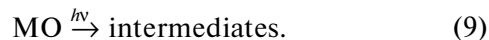
Fig. 2. Effect of anions on the mineralization degree of the combined $UV/S_2O_8^{2-}/Fe^{2+}$ system: $[Fe^{2+}] = 180\ \mu M$, $[S_2O_8^{2-}] = 180\ \mu M$. The radiation dose was $1.48\ J\ cm^{-2}$; S is salinity.

At the first step of the reaction between methyl orange and ROS, the azo bond is cleaved and nitro compounds are produced. Subsequent oxidation includes the formation of polyatomic nitrophenols, the opening of aromatic rings, the decarboxylation of carboxylic acids, and the evolution of carbon dioxide [26, 27].

Adding hydrocarbonates buffers a solution (Table 1). This is accompanied by the hydrolysis of Fe^{2+} ions, their deactivation, and chain termination in Fenton-like $UV/S_2O_8^{2-}/Fe^{2+}$ oxidation. At the same time, there is needless consumption of ROSes, due to the high rate of their interaction with hydrocarbonates
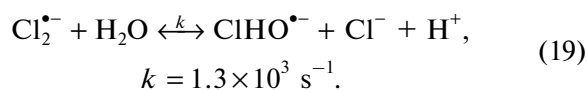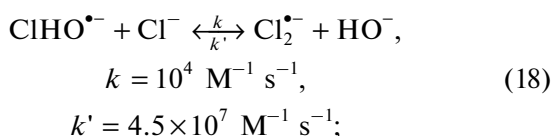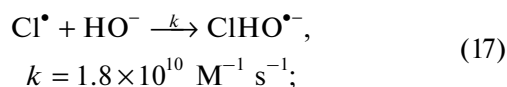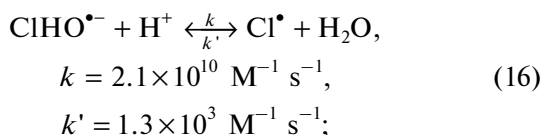
$$SO_4^{-\bullet} + HCO_3^- \rightarrow SO_4^{2-} + CO_3^{\bullet-} + H^+,$$
$$k = 2.8 \times 10^6\ M^{-1}\ s^{-1}\ [19]; \tag{10}$$

$$OH^\bullet + HCO_3^- \rightarrow CO_3^{\bullet-} + H_2O,$$
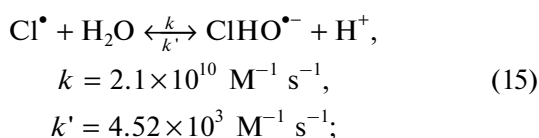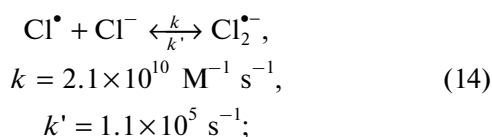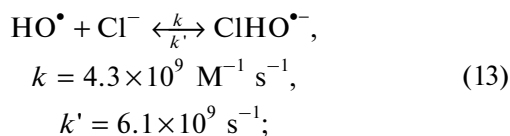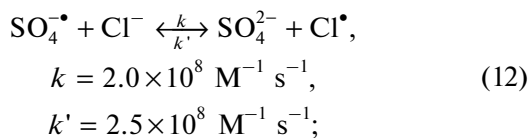$$k = 8.6 \times 10^6\ M^{-1}\ s^{-1}\ [19]. \tag{11}$$

Data on the effect chlorides have on the oxidative destruction of aqua pollutants in combined systems based on using persulfates as oxidants are contradictory. Many studies have noted the inhibitory effect of chlorides, especially at high concentrations of them [28, 29]. This is because chlorides can also react at high rates with hydroxyl radicals and sulfate radical anions produced in solutions, after which they act as radical traps (reactions (12) and (13)). Upon the activation of persulfate using Fe^{2+} ions, chlorides can

form stable complexes with Fe^{3+}, thereby terminating the cycle of iron reduction in the catalytic system. It has been confirmed experimentally [30, 31] that upon oxidating a mixture of organic compounds containing benzene, toluene, ethylbenzene, and xylenes with thermally activated persulfate, the effect of chlorides is governed by both the nature of the oxidized substance and the concentration of anions.

It has been established experimentally that chlorides at concentrations of up to 1 mM have no effect on the rate of oxidation of MO or the mineralization degree of DOC in the combined $UV/S_2O_8^{2-}/Fe^{2+}$ system (Figs. 1 and 2). A further increase in the concentration of chlorides is accompanied by a slight drop in the initial rates of oxidation of MO, but the radiation dose required for the complete conversion of MO is almost unchanged. It should be noted, however, that mineralization degree grows considerably (from 31 to 50%) at a chloride concentration of 10 mM (Fig. 2).

A similar effect has been observed for the oxidation of sulphamethoxazole, carbamazepine, and bisphenol-A upon activating persulfate and peroxomonosulfate with UV radiation [30, 31]. Laser flash photolysis was used to prove experimentally that chlorine-containing radicals $ClOH^{\bullet-}$, $Cl^\bullet$, and $Cl_2^{\bullet-}$ are produced in a solution, due presumably to reactions (12)−(19) [12]. Quantum chemical calculations showed that chlorides lower the energy of activation of the forma-

tion of sulfate radical anions from persulfates [32], which can also raise the mineralization degree of DOC:

$$SO_4^{-\bullet} + Cl^- \xleftrightarrow[k']{k} SO_4^{2-} + Cl^\bullet,$$
$$k = 2.0 \times 10^8 \ M^{-1} \ s^{-1}, \tag{12}$$
$$k' = 2.5 \times 10^8 \ M^{-1} \ s^{-1};$$

$$HO^\bullet + Cl^- \xleftrightarrow[k']{k} ClHO^{\bullet-},$$
$$k = 4.3 \times 10^9 \ M^{-1} \ s^{-1}, \tag{13}$$
$$k' = 6.1 \times 10^9 \ s^{-1};$$

$$Cl^\bullet + Cl^- \xleftrightarrow[k']{k} Cl_2^{\bullet-},$$
$$k = 2.1 \times 10^{10} \ M^{-1} \ s^{-1}, \tag{14}$$
$$k' = 1.1 \times 10^5 \ s^{-1};$$

$$Cl^\bullet + H_2O \xleftrightarrow[k']{k} ClHO^{\bullet-} + H^+,$$
$$k = 2.1 \times 10^{10} \ M^{-1} \ s^{-1}, \tag{15}$$
$$k' = 4.52 \times 10^3 \ M^{-1} \ s^{-1};$$

$$ClHO^{\bullet-} + H^+ \xleftrightarrow[k']{k} Cl^\bullet + H_2O,$$
$$k = 2.1 \times 10^{10} \ M^{-1} \ s^{-1}, \tag{16}$$
$$k' = 1.3 \times 10^3 \ M^{-1} \ s^{-1};$$

$$Cl^\bullet + HO^- \xrightarrow{k} ClHO^{\bullet-},$$
$$k = 1.8 \times 10^{10} \ M^{-1} \ s^{-1}; \tag{17}$$

$$ClHO^{\bullet-} + Cl^- \xleftrightarrow[k']{k} Cl_2^{\bullet-} + HO^-,$$
$$k = 10^4 \ M^{-1} \ s^{-1}, \tag{18}$$
$$k' = 4.5 \times 10^7 \ M^{-1} \ s^{-1};$$

$$Cl_2^{\bullet-} + H_2O \xleftrightarrow{k} ClHO^{\bullet-} + Cl^- + H^+,$$
$$k = 1.3 \times 10^3 \ s^{-1}. \tag{19}$$

The effect nitrates have on the oxidation of organic compounds by persulfates depends on how they are activated. For example, it was found that nitrates at concentrations of 10–500 mM have no appreciable effect on the oxidation of a mixture of organic compounds consisting of benzene, toluene, ethylbenzene, and xylenes with thermally activated persulfates [20]. At the same time, it is known that nitrates can have a dual effect on the course of photocatalytic reactions. On the one hand, nitrates can absorb ultraviolet radiation (at $\lambda = 205$ nm, $\varepsilon = 9900 \ M^{-1} \ cm^{-1}$ [33]), which prevents light from penetrating to the bulk of a solution. On the other hand, nitrates exposed to UV radiation in an aqueous solution can serve to form hydroxyl and nitrite radicals or superoxide radical anions, which raises the total oxidation potential of the system:

$$NO_3^- + h\nu \rightarrow NO_2^\bullet + O^{\bullet-}, \tag{20}$$

$$O^{\bullet-} + H_2O \rightarrow {}^\bullet OH + OH^-. \tag{21}$$
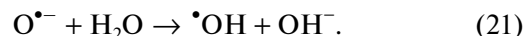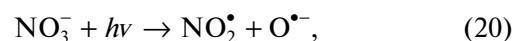
However, the contribution from reactions (20) and (21) to oxidation becomes appreciable only when using vacuum UV radiation ($\lambda < 200$ nm) [34].

In our combined $UV/S_2O_8^{2-}/Fe^{2+}$ system, nitrates had no appreciable effect on the kinetics of MO oxidation (Fig. 1). However, the mineralization of DOC fell considerably (from 31 to 6%) upon raising the concentration of nitrates from 1 to 100 mM, due mainly to an increase in the contribution from the shielding effect that lowered the total oxidation potential of the system (Fig. 2).

We studied the effect sulfates have on the photochemical oxidation of MO in the combined $UV/S_2O_8^{2-}/Fe^{2+}$ system. It was found experimentally that in the presence of sulfate ions, the radiation dose required for the complete conversion of MO in the considered range of concentrations remained almost unchanged. However, the mineralization degree of DOC rose to 56–61%.

A similar intensifying effect of sulfates has been observed during the oxidative destruction of chloramphenicol with photoactivated persulfate [35]. The authors assumed that when there are sulfates in a solution, the probability of needless reactions that lead to the consumption of ROSes (including ones between sulfate radical anions and persulfate) falls

$$SO_4^{\bullet-} + S_2O_8^{2-} \rightarrow S_2O_8^{2-\bullet} + SO_4^{2-}. \tag{22}$$
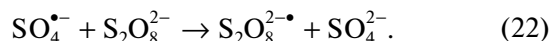
Even though sulfates do not react with sulfate radical anions [20], they can indirectly generate additional amounts of $SO_4^{\bullet-}$ via the reaction [36]

$$HO^\bullet + SO_4^{2-} \rightarrow SO_4^{\bullet-} + OH^-. \tag{23}$$
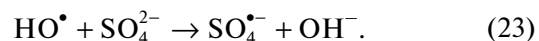
Effect of Components of Real Aqueous Matrices

The destruction of micropollutants in combined oxidation systems in aqueous matrices of multicomponent natural and waste waters proceed much more slowly, and depend not only on the concentration of anions but on their mutual effect as well [37].

The components of two aqueous matrices (natural surface water of the Selenga River and the wash water from dyeing fur black) were found experimentally to affect the kinetics of oxidation of MO in the combined $UV/S_2O_8^{2-}/Fe^{2+}$ system. The initial rate of oxidation of MO in the natural water fell from 6.1 to 1.5 $\mu M \ min^{-1}$, the efficiency of dye oxidation at a radiation dose of 1.48 J cm^{-2} was only 50%, and no mineralization of DOC was observed (Fig. 3).
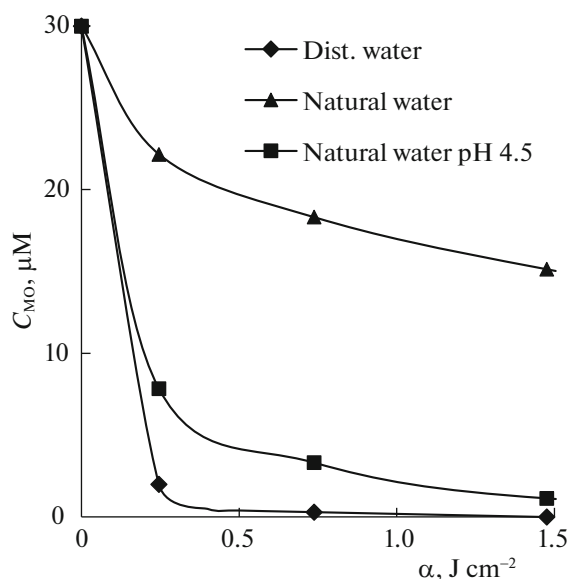
Fig. 3. Kinetics of the photochemical oxidation of MO in natural water: $[Fe^{2+}] = 180\ \mu M$, $[S_2O_8^{2-}] = 180\ \mu M$.

We assume the reduced efficiency of MO oxidation in this matrix was mainly due to the presence of hydrocarbonates (76 mg/L), since the pattern of the kinetic curve correlates well with the above data on the oxidation of MO in model solutions (distilled water) in the presence of hydrocarbonates.

Experiments with the initial pH of the medium adjusted to 4.5 were performed to mitigate the inhibi-tory effect of HCO_3^-. The initial rate of MO oxidation rose to 4.43 $\mu M\ min^{-1}$, the efficiency of oxidation was 99%, and the mineralization degree of DOC reached 35%.

Wash waters from fur dyeing have a complex multi-component composition that includes (in addition to dyes) residual concentrations of process impurities and reagents used in the production of dye baths (e.g., levelers, organic acids, and surfactants). This results in high contents of oxidation-resistant impurities (COD = 420 mg/L O_2) and DOC (210 mg/L).

The efficiency of using the combined $UV/S_2O_8^{2-}/Fe^{2+}$ oxidation system to purify fur dyeing wash waters was estimated from the change in the characteristic indices of water quality, the COD, and the concentration of DOC. Under the optimum conditions determined for model solutions, the efficiency of MO oxidation was 83% at an absorbed radiation dose of 5.9 J cm^{-2}. Min-eralization degree was 24%, and COD fell by 7% (Figs. 4 and 5). Doubling the concentration of the oxi-dizer intensified the destruction of reaction products, as is seen from the considerable drop in the COD (60%) (Fig. 6). The specific consumption of the oxi-dizer was in this case 0.7 μmol of $S_2O_8^{2-}$ per gram of removed COD. We do not advise raising the concen-tration of persulfate further, since this results in its nontargeted consumption (Fig. 5).

CONCLUSIONS

We studied the effect the anions (hydrocarbonates, chlorides, nitrates, and sulfates) most typical of natu-
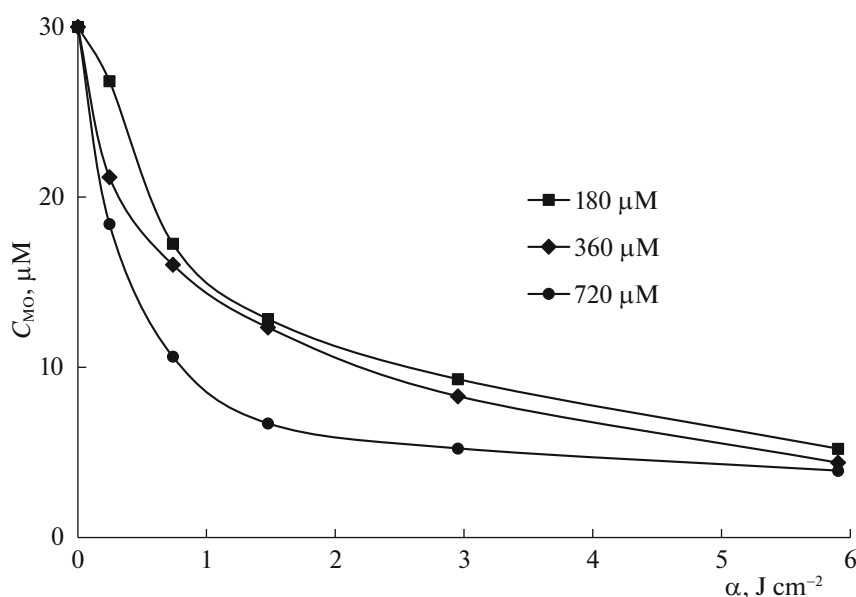

Fig. 4. Effect of the concentration of oxidizer on the change in the concentration of dye in the wash waters of fur dyeing: $[Fe^{2+}] = 180\ \mu M$.

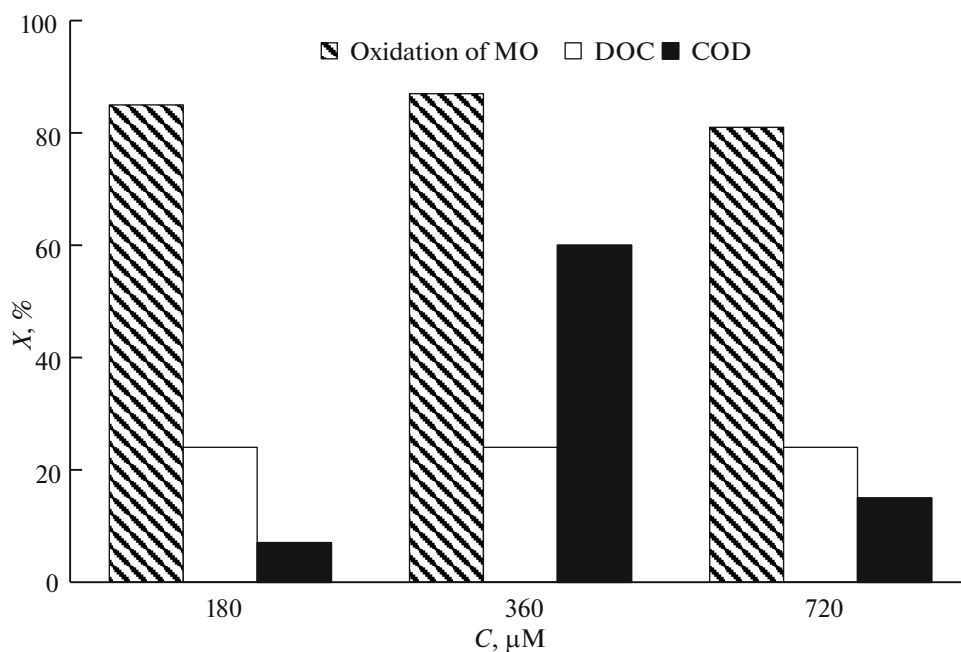**Fig. 5.** Effect of the concentration of oxidizer (C) on the efficiency (X) of purifying wash waters of fur dyeing in the combined UV/$S_2O_8^{2-}$/Fe^{2+} oxidation system: [Fe^{2+}] = 180 μM; radiation dose, 5.9 J cm^{-2}.

ral and waste waters have on the kinetics of oxidation of methyl orange in a combined UV/$S_2O_8^{2-}$/Fe^{2+} system using a KrCl exilamp (222 nm) as the UV source. Adding hydrocarbonates and nitrates to a solution was found to inhibit the mineralization of dissolved organic carbon. The mineralization degree rose from 31 to 60% using chlorides (10 mM) and sulfates (1–100 mM). Oxidation is inhibited considerably in real aqueous matrices (natural water and waste water from fur dyeing). In natural surface water, this effect is due to the predominance of hydrocarbonates. In waste water, it is associated with the multicomponent pattern of an aqueous matrix containing process impurities.

Fig. 6. Efficiency of purifying wash waters from fur dyeing in the combined UV/$S_2O_8^{2-}$/Fe^{2+} oxidation system: [Fe^{2+}] = 180 μM; [$S_2O_8^{2-}$] = 360 μM.

REFERENCES

1. A. Babuponnusami and K. Muthukumar, Chem. Eng. J. **183**, 1 (2012).
2. A. Sharma, J. Ahmad, and S. J. S. Flora, Environ. Res. **167**, 223 (2018).
3. D. S. Babu, V. Srivastava, P. V. Nidheesh, and M. S. Kumar, Sci. Total Environ. **696**, 133961 (2019).
4. D. B. Miklos, Ch. Remy, M. Jekel, et al., Water Res. **139**, 118 (2018).
5. M.-H. Zhang, H. Dong, L. Zhao, et al., Sci. Total Environ. **670**, 110 (2019).
6. A. Karci, I. Arslan-Alaton, T. Olmez-Hanci, and M. Bekbölet, J. Photochem. Photobiol. A **230**, 65 (2012).
7. J. Méndez-Díaz, M. Sánchez-Polo, J. Rivera-Utrilla, et al., Chem. Eng. J. **163**, 300 (2010).
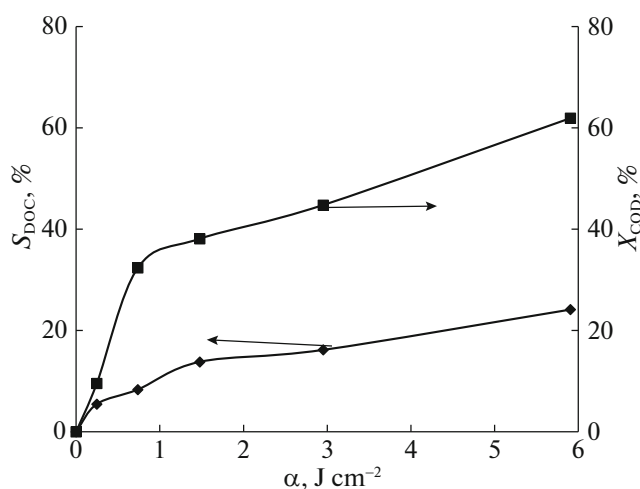8. H. Mestankova, K. Schirmer, S. Canonica, and U. von Gunten, Water Res. **66**, 399 (2014).

9. A. R. Ribeiro, N. F. F. Moreira, G. L. Puma, and A. M. T. Silva, Chem. Eng. J. **363**, 155 (2019).

10. R. Matta, S. Tlili, S. Chiron, et al., Environ. Chem. Lett. **9**, 347 (2011).

11. F. Ghanbari and M. Moradi, J. Hazard. Mater. **310**, 41 (2017).

12. W. Huang, A. Bianco, M. Brigante, and G. Mailhot, J. Hazard. Mater. **347**, 279 (2018).

13. L. Matzek and K. E. Carter, Chemosphere **151**, 178 (2016).

14. I. A. Ike, K. G. Linden, J. D. Orbell, and M. Duke, Chem. Eng. J. **338**, 651 (2018).

15. Q. Yang, Y. Ma, F. Chen, et al., Chem. Eng. J. **378**, 1221499 (2019).

16. G. Matafonova and V. Batoev, Water Res. **132**, 177 (2018).

17. G. Matafonova and V. Batoev, Chemosphere **89**, 637 (2012).

18. Y. Fu, G. Wu, J. Geng, et al., Water Res. **150**, 12e2013 (2019).

19. C. Luo, J. Ma, J. Jiang, et al., Water Res. **80**, 99 (2015).

20. J. Ma, Y. Yang, X. Jiang, et al., Chemosphere **190**, 296 (2018).

21. M. Sizykh and A. Batoeva, Russ. J. Phys. Chem. A **93**, 2349 (2019).
https://doi.org/10.1134/S003602441912029X

22. S. Canonica, L. Meunier, and U. Gunten, Water Res. **42**, 121 (2008).

23. J. Ma and N. J. D. Graham, Water Res. **34**, 3822 (2000).

24. E. Brillas and C. A. Martínez, Appl. Catal. B **166−167,** 603 (2015).

25. F. C. Moreira, S. Garcia-Segura, V. J. P. Vilar, et al., Appl. Catal. B **142−143,** 877 (2013).

26. Q. Qin, J. Xu, T. Sun, et al., Res. Chem. Intermed. **45**, 3541 (2019).

27. J. M. Joseph, H. Destaillats, H.-M. Hung, and M. R. Hoffmann, J. Phys. Chem. A **104**, 301 (2000).

28. W. L. Bi, Y. L. Wu, X. N. Wang, et al., Chem. Eng. J. **302**, 811 (2016).

29. J. Sharma, I. M. Mishra, D. D. Dionysiou, and V. Kumar, Chem. Eng. J. **276**, 193 (2015).

30. X. W. Ao and W. J. Liu, Chem. Eng. J. **313**, 629 (2017).

31. J. Deng, Y. S. Shao, N. Y. Gao, et al., Chem. Eng. J. **222**, 150 (2013).

32. R. Zhang, X. Wang, L. Zhou, and D. Crump, Chem. Eng. J. **361**, 960 (2019).

33. J. Mack and J. R. Bolton, J. Photochem. Photobiol. A **128**, 1 (1999).

34. M. Han and M. Mohseni, Water Res. **168**, 115169 (2020).

35. A. Ghauch, A. Baalbaki, M. Amasha, E. R. Asmar, et al., Chem. Eng. J. **317**, 1012 (2017).

36. M. G. Antoniou, A. A. de la Gruz, and D. D. Dionysiou, Appl. Catal. B **96**, 290 (2010).

37. S. Al Hakim, S. Jaber, N. Z. Eddine, and J. Xu, Chem. Eng. J. **380**, 1224782 (2020).

Translated by K. Utegenov